

RSC Advances



This is an *Accepted Manuscript*, which has been through the Royal Society of Chemistry peer review process and has been accepted for publication.

Accepted Manuscripts are published online shortly after acceptance, before technical editing, formatting and proof reading. Using this free service, authors can make their results available to the community, in citable form, before we publish the edited article. This *Accepted Manuscript* will be replaced by the edited, formatted and paginated article as soon as this is available.

You can find more information about *Accepted Manuscripts* in the [Information for Authors](#).

Please note that technical editing may introduce minor changes to the text and/or graphics, which may alter content. The journal's standard [Terms & Conditions](#) and the [Ethical guidelines](#) still apply. In no event shall the Royal Society of Chemistry be held responsible for any errors or omissions in this *Accepted Manuscript* or any consequences arising from the use of any information it contains.

Synthesis and Biological Evaluation of Copper(II)

Pyrenethiosemicarbazone

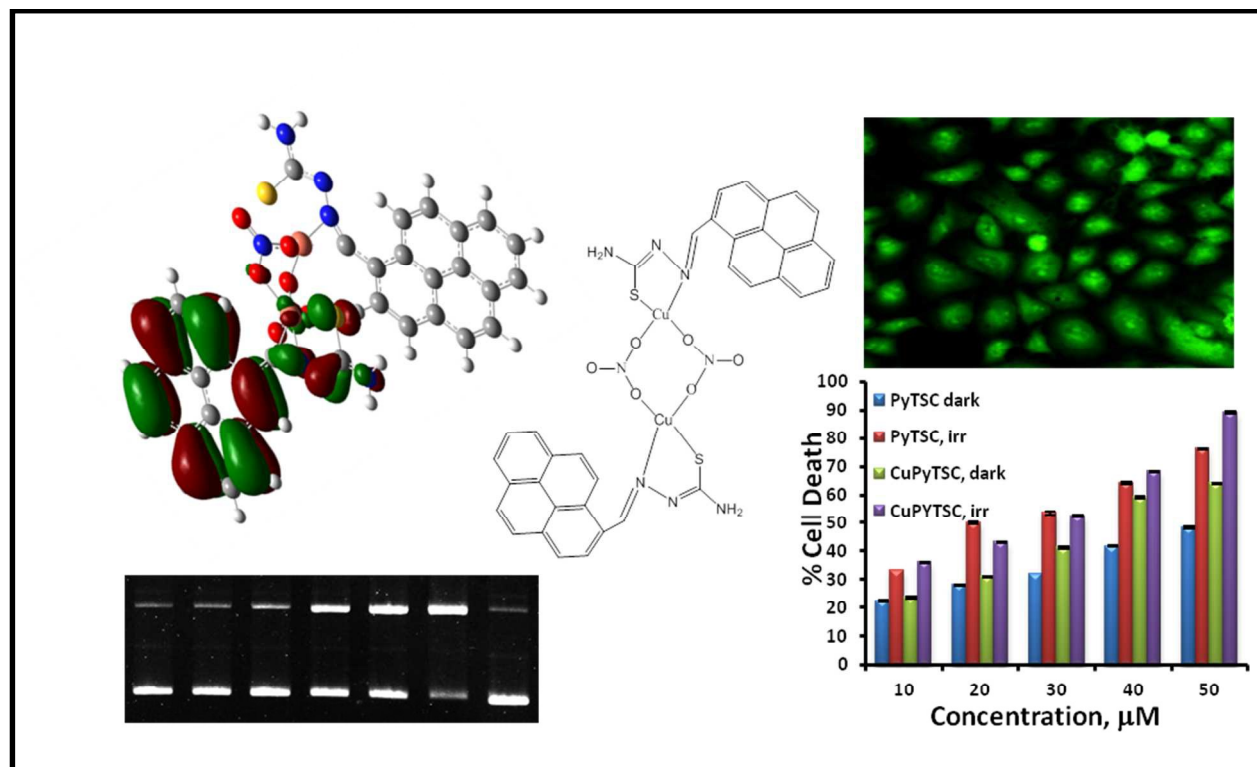
Suwarna A. Ingle, Anup N. Kate, Anupa A. Kumbhar,* Ayesha A. Khan,

Soniya S. Rao and Shridhar P. Gejji

Department of Chemistry, Savitribai Phule Pune University, Pune- 411007, India.

Table of Contents

A fluorescent Cu(II) pyrenethiosemicarbazone complex exhibits enhanced DNA-cleavage and cytotoxicity on photoexcitation.



Synthesis and Biological Evaluation of Copper(II) Pyrenethiosemicarbazone

Suwarna A. Ingle, Anup N. Kate, Anupa A. Kumbhar,* Ayesha A. Khan,
Soniya S. Rao and Shridhar P. Gejji

Department of Chemistry, Savitribai Phule Pune University, Pune- 411007, India.

*Corresponding author:

E-mail: aak@chem.unipune.ac.in

Fax: +91-020-25691728; Tel: +91-020-25601395/97 Ext. 516

Abstract

Pyrenethiosemicarbazone (PyTSC) and its copper(II) complex (CuPyTSC) have been synthesized and characterized by elemental analysis, $^1\text{H-NMR}$, IR, ESI-MS, cyclic voltammetry, UV-Visible and fluorescence spectroscopy. Both the compounds interact with calf thymus (CT) DNA via intercalation with apparent binding constant, K_b , of the order of 10^5 . CuPyTSC shows photo-induced DNA cleavage of plasmid pBR322 DNA (74%) than PyTSC (14%). Mechanistic investigations revealed involvement of singlet oxygen species in the DNA cleavage by both the compounds. DFT calculations demonstrated more efficient generation of singlet oxygen by CuPyTSC with decreased HOMO-LUMO gap (0.332 eV) than PyTSC (0.629 eV). The protein binding ability has been monitored using Bovine Serum Albumin (BSA). The compounds show green fluorescence revealing their uptake by the cells under fluorescence microscope. CuPyTSC displayed better cytotoxic activity on photoexposure on B16F10 melanoma cells.

1. Introduction

Thiosemicarbazones (TSCs) and their transition metal complexes have received significant attention in coordination and medicinal chemistry due to their anti-inflammatory, antibacterial, antimalarial, antioxidant and analgesic activities.¹⁻⁷ This class of N, S donor ligands with variable donor abilities yielded structurally diverse mono-, di-, tri- and polynuclear complexes mainly because thiosemicarbazones can coordinate in either anionic or neutral form.⁸ The type of anion, nature of aldehyde, coligands, solvent, etc. further govern the bonding characteristics and nuclearity of the complexes.⁹⁻²¹ A wide range of thiosemicarbazone derivatives and their transition metal complexes endowed with rich coordination chemistry have been reported in the literature in last two decades with emphasis on DNA-binding, DNA cleavage, and anticancer/ antitumor activities.²²⁻³⁴ The underlying molecular interactions bring about either DNA damage or inhibition of ribonucleotide reductase and topoisomerase II enzymes which block the cell division leading to cell death.³⁵⁻³⁸ Different strategies have been adopted for designing of the drugs to suit a particular application. Neutral Cu(II)-bis(thiosemicarbazone) complexes have shown selectivity to hypoxic cells compared to normal cells.³⁹⁻⁴¹ It has further been demonstrated that subtle changes in the backbone of ligand dramatically alters the biological activity of these complexes^{42,43} which are used as blood flow tracers in brain, kidney and heart, inhibiting the DNA and RNA synthesis.^{44,45} These complexes can be utilized as theranostics allowing simultaneous diagnosis and therapy.⁴⁶⁻⁵⁰ A recent review by Dilworth and Hueting summarizes the applications of coordination complexes of tridentate and tetradentate thiosemicarbazones in therapeutic and/or diagnostic PET/ SPECT imaging.⁵¹

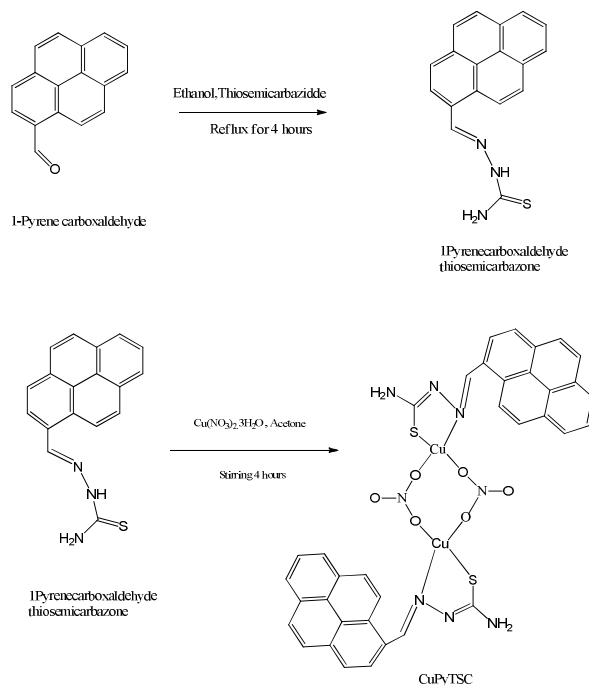
The discovery that DNA is the cellular target of cisplatin has led to investigations into the mechanism of action of several platinum and non-platinum anticancer compounds. A large

number of the copper complexes are reported as chemical nucleases wherein the DNA cleavage occurs either by oxidative or hydrolytic mechanisms.⁵²⁻⁶⁸ In this regard, the number of copper complexes showing photo-induced DNA cleavage activity are relatively small⁶⁹⁻⁷⁴ and by including an appropriate photosensitizer in a ternary system the activity can be improved significantly. Since copper (II) complexes are intrinsically non-fluorescent, tagging them with fluorescent probes can provide insights into their entry, distribution and localization inside the cell organelles using fluorescence microscopy.⁷⁵⁻⁷⁷ Thus, development of dual modality imaging/ therapeutic agents to induce DNA cleavage and/or cell death besides monitoring cellular uptake will be beneficial.⁷⁸⁻⁸³ This strategy was used by Holland and coworkers⁸⁴ who demonstrated that pyrene functionalized Cu(II) complexes can be utilized as *in vitro* fluorescence imaging agents.

Besides wide pharmacological properties, the choice of thiosemicarbazone is based on its ability to act as a photosensitizer. It has been shown that thio- or thione containing moieties like TSCs display efficient intersystem crossing on photo-irradiation with longer excited state lifetimes thereby producing singlet oxygen species.^{70-74,85,86} Our interest in pyrene is due to its high fluorescence and planar aromatic structure which can intercalate into DNA. In addition, pyrene has been shown to be more selective triplet photosensitizer.⁸⁷ It has been shown that bichromophoric compounds containing pyrene and benzoylthiophene moieties are a robust triplet photosensitizers with efficient intersystem crossing and enhanced selectivity towards photocatalysis of E-stilbene.⁸⁸

With the view that amalgamation of thiosemicarbazone and pyrene moieties would lead to a conjugate with enhanced photosensitizing ability coupled with high emission intensity and improved cytotoxicity, the present work focuses on the synthesis of pyrenethiosemicarbazone

(PyTSC) and its copper(II) complex (CuPyTSC). The compounds have been isolated and characterized by elemental analysis, $^1\text{H-NMR}$, ESI-MS, cyclic voltammetry, IR, UV-Visible and fluorescence spectroscopy. Their DNA binding, DNA-cleavage and protein binding efficacy and cellular uptake and cytotoxicity profile on B16F10 melanoma cells has been evaluated. Density functional theoretical studies have been carried out to gauge the photosensitizing abilities.



Scheme 1 Synthesis of 1-pyrenecarboxaldehyde thiosemicarbazone and its copper(II) complex.

2. Experimental Section

2.1 Materials and Methods:

Copper nitrate and thiosemicarbazide (AR grade, SD Fine Chemicals India), Pyrenecarboxaldehyde (Sigma Aldrich), HPLC grade DMF, Bovine Serum Albumin (fraction V) and Analytical Reagent Grade KH_2PO_4 and K_2HPO_4 (SRL India) and plasmid pBR 322 DNA (Chromos Biotech, India) were obtained and used as received. All the reagents used for the synthesis were free from impurities.

UV-VIS and fluorescence spectra were measured on a Shimadzu UV-1601 Spectrophotometer and JASCO FP-8200 spectrofluorimeter, respectively. The infrared spectra of solid samples dispersed in KBr were recorded on a Shimadzu FTIR-8400 spectrophotometer. ^1H NMR spectra were obtained on a Varian-Mercury 300 MHz spectrometer with DMSO-d_6 as solvent at room temperature and all chemical shifts are calculated relative to TMS. The elemental analyses in positive ion mode were carried out on Thermoelectron Corporation, model 1112. Electrospray ionization mass spectral measurements were performed on Bruker Nano-Advance UHPLC-MS-MS with TOF analyzer (PyTSC) and Thermo Finnigan LCQ Advantage max ion trap mass spectrometer (CuPyTSC).

2.2 Synthesis of 1-Pyrenethiosemicarbazone (PyTSC)

The ligand 1-pyrenethiosemicarbazone (PyTSC) was synthesized as per the reported procedure.⁸⁹ Thiosemicarbazide (0.52 mmol, 47.38 mg) and pyrenecarboxaldehyde (0.43 mmol, 100 mg) were refluxed in ethanol (1% acetic acid) for 4 h. The yellow product obtained was filtered, recrystallized and dried over fused CaCl_2 . Yield= 80%. ^1H NMR (300 MHz, DMSO-d_6): δ 11.596 (s, 1H, NH), 9.289 (s, 1H, CH=), 8.936 (d, 1H), 8.51-8.113 (m, 8H of pyrene). IR (KBr, $\nu \text{ cm}^{-1}$): 3439 (NH_2 , asymmetrical stretching), 3273 (NH_2 , symmetrical stretching), 3153 (pyrene H), 1600 (C=N), 1541 (=CN), 711 (C=S). UV-Visible $\lambda_{\text{max}} = 280, 370, 420 \text{ nm}$. Fluorescence ($\lambda_{\text{ex}} = 370 \text{ nm}$) $\lambda_{\text{em}} = 476 \text{ nm}$. Elemental analysis for $\text{C}_{18}\text{H}_{13}\text{N}_3\text{S}$: calculated (%), C 71.26, H 4.31, N 13.85; Found C 70.78, H 4.27, N 13.08; ESI-MS (m/z) : $[\text{M} + \text{K}]^+ = 342.0498$.

2.3 Synthesis of $[\text{Cu}(\text{PyTSC})\text{NO}_3]_2$ complex (CuPyTSC)

The $\text{Cu}(\text{NO}_3)_2 \cdot 3\text{H}_2\text{O}$ (0.16 mmol, 39.81 mg) was slowly added to the solution of PyTSC (0.32 mmol, 100 mg) in acetone and stirred for $\sim 4 \text{ h}$. Brown coloured complex was obtained in 82% yield. IR (KBr, $\nu \text{ cm}^{-1}$): (NH_2 , asymmetrical stretching), 3273 (NH_2 , symmetrical

stretching), 3153 (pyrene H), 1796 and 1740 ($\Delta\nu = 56$, bidentate bridging mode of nitrate), 1622 (C=N), 1541 (=CN), 713 (C=S). Fluorescence ($\lambda_{\text{ex}} = 370$ nm) $\lambda_{\text{em}} = 450$ nm. Elemental analysis for $\text{C}_{36}\text{H}_{24}\text{N}_8\text{O}_6\text{S}_2\text{Cu}_2\cdot\text{CH}_3\text{COCH}_3\cdot\text{H}_2\text{O}$: calculated (%), C 50.26, H 3.46, N 13.64; found C 50.85, H 3.71, N 8.57. ESI-MS (m/z) : $[\text{M} + \text{Acetone}]^+ = 912.3$, $[\text{M}^+ - \text{NO}_2] = 808.2$.

2.4 DNA Binding

The CT-DNA binding experiments were performed in phosphate buffer (pH 7.2) using 10% DMF solution of PyTSC and CuPyTSC. The concentration of CT DNA was calculated from its absorption intensity at 260 nm ($\epsilon = 6600 \text{ M}^{-1} \text{ cm}^{-1}$). A ratio of UV absorbance at 260 and 280 nm of a solution of CT DNA was found to be 1.8:1, suggesting that the DNA was sufficiently free from protein. Intrinsic binding constant was calculated using equation (1):

$$[\text{DNA}] / [\epsilon_a - \epsilon_f] = [\text{DNA}] / [\epsilon_b - \epsilon_f] + 1 / K_b [\epsilon_b - \epsilon_f] \quad (1)$$

where $[\text{DNA}]$ refers to the concentration of DNA in base pairs, ϵ_a , extinction coefficient observed for the absorption band at the given DNA concentration, ϵ_f , extinction coefficient of the complex free in solution, and ϵ_b is the extinction coefficient of the complex when fully bound to DNA. A plot of $[\text{DNA}] / [\epsilon_a - \epsilon_f]$ versus $[\text{DNA}]$ gave a slope $1 / [\epsilon_a - \epsilon_f]$ and Y intercept equal to $(1/K_b) [\epsilon_b - \epsilon_f]$, respectively. The ratio of the slope to the intercept gave intrinsic binding constant, K_b .

Ethidium bromide (EB) quenching experiments were carried out by the successive addition of 0-50 μM of PyTSC and CuPyTSC to CT-DNA (10 μM) solutions containing 10 μM ethidium bromide (EB) in phosphate buffer. The changes in fluorescence intensities were measured at 585 nm (545 nm excitation) of EB bound to DNA.

2.5 Viscosity measurements

Viscosity measurements were carried out using a semi-microviscometer maintained at 28°C in a thermostatic water bath. Flow time of solutions in phosphate buffer (pH 7.2) was recorded in triplicate for each sample and an average flow time was calculated. Data were presented as $(\eta/\eta_0)^{1/3}$ versus binding ratio, where η is the viscosity of DNA in the presence of complex and η_0 is the viscosity of DNA alone.

2.6 DNA Cleavage:

DNA cleavage was studied on 1% agarose gel electrophoresed for 3 h at 60 V. Supercoiled pBR 322 DNA was treated with the PyTSC and CuPyTSC (10-50 μ M) and the mixture was incubated for 30 min in dark followed by 20 min irradiation at 365 nm (monochromatic light). The gel was stained with a 0.5 μ g/mL ethidium bromide and visualized by UV light and photographed for analysis. The extent of cleavage of the SC DNA was determined by measuring the intensities of the bands using the Alpha Innotech Gel Documentation System (AlphaImager 2200).

Cyclic voltammetric experiments were performed on a CH-electrochemical analyzer model 1100A with a conventional three-electrode cell assembly with a saturated Ag/AgCl reference electrode, glassy carbon electrode as working electrode and platinum wire as an auxiliary electrode in the presence of tetrabutylammonium perchlorate as supporting electrolyte in dimethyl formamide. The solutions were degassed for 1 h and blanketed with N₂ prior to measurements.

Emission quantum yields (Φ) were calculated by integrating the area under the fluorescence curves and by using the following formula

$$\Phi_{\text{Sample}} = \left\{ \frac{\text{OD}_{\text{Standard}}}{\text{OD}_{\text{Sample}}} \right\} \times \left\{ \frac{A_{\text{Sample}}}{A_{\text{Standard}}} \right\} \times \Phi_{\text{Standard}} \quad (2)$$

where OD is optical density of the compound at the excitation wavelength (370 nm) and A is the area under the emission spectral curve. Pyrenecarboxaldehyde was used as a standard for the fluorescence quantum yield measurements.⁹⁰

2.7 Computational Method

Optimized structures of Pyrenealdehyde (Py), Thiosemicarbazone (TSC), PyTSC, CuPyTSC were derived within the framework of density functional theory incorporating the Becke's correlation functional coupled with 3-parameter exchange given by Lee, Yang and Parr (B3LYP).^{91,92} The charge distributions in terms of Frontier orbitals have been derived for the stationary point structures using the Gaussian-09 program⁹³ with the internally stored 6-31G (d,p) basis set.

2.8 BSA Interaction

Quenching of tryptophan residues of BSA were studied using PyTSC and CuPyTSC as quencher. The titration was carried out in phosphate buffer of pH 7.2. The emission signals were recorded at 340 nm and the excitation wavelength was 295 nm.

2.9 Cellular uptake and cytotoxicity

In vitro cellular uptake of PyTSC and CuPyTSC was monitored using fluorescence microscope. Surface sterilized coverslips were kept in 6-well plates. B16F10 cells were cultured in these plates for 24 h which grew on the pre-laid coverslips, before addition of medium containing fluorescent compounds. This was followed by incubation for another 8 h in dark and images were recorded. Similarly, the cells were exposed to monochromatic UV-light of 365 nm immediately after addition of the compounds and further incubated till 8 h before recording the images. Photographs of control cells were also recorded on incubation in dark and on photoexposure in a similar way to that of compounds to evaluate the effect of radiation on cells.

To test the efficacy of the compounds on long term cell growth inhibition and cell proliferation the compounds were dissolved in 5% DMSO and added to the cells seeded in 96-well plates at different concentrations. The control well contained 5% DMSO and considered during cell death calculations. The cytotoxicity was evaluated after 48 h incubation by the MTT assay performed in triplicates.

5 mg MTT was dissolved in 1 mL PBS and filter sterilized using syringe filter. After incubation for the stipulated time, 20 μL of MTT solution was added to 200 μL of cell content solution. The plate was incubated for 2 h in the CO_2 incubator. After incubation, the media was removed and 200 μL DMSO was added to each well to dissolve the crystals. The plate was incubated for another 5 min at 37°C before reading for absorbance at 540 and 620 nm on Thermo Electron Corporation multiplate reader.

3 Results and Discussion

3.1 Synthesis and Characterization

Scheme 1 depicts the synthetic route of ligand pyrenethiosemicarbazone and its Cu(II) complex. The ^1H NMR spectrum of PyTSC recorded in DMSO-d_6 solvent reveals peak at 11.59 ppm assigned to the azomethinic H-N. Peak at 9.29 is assigned to CH in TSC while peaks in the range 8.94 to 8.11 are assigned to the pyrene protons. The copper complex was prepared by direct reaction of ligand with copper nitrate in acetone in 2:1 molar ratio. It was characterized by elemental analysis, IR, UV-Vis, fluorescence and mass spectroscopy. Elemental analysis of the complex indicates formation of a dimeric copper(II) complex bridged by two nitrates⁹⁴⁻⁹⁶ as depicted in Scheme 1. The mass spectrum of PyTSC shows a peak at $m/z = 342.0498$ which corresponds to $[\text{M} + \text{K}]^+$. Cu(II) complex shows a molecular ion peak at $m/z = 912.3$ corresponding to $[\text{M}^+ + \text{acetone}]$ and a base peak at $m/z = 808.2$ which matches to $[\text{M}-\text{NO}_2]^+$

species. IR spectrum of PyTSC showed symmetric and asymmetric stretching vibrations of NH_2 at 3439 and 3273 cm^{-1} respectively (Table 2). The coordination mode of nitrate is also evident in the IR spectrum of CuPyTSC. Frequency difference of vibrations $\Delta\nu = 56$ ($\Delta\nu = 1796-1740 \text{ cm}^{-1}$) indicate a bidentate, bridging coordination mode of nitrates.⁹⁴⁻⁹⁶ The C=S and C=N frequencies appear at 711 and 1600 cm^{-1} respectively. In CuPyTSC all the peaks in IR were observed at the same position except C=N and C=S, which were slightly shifted and observed at 1622 and 713 cm^{-1} respectively, indicating the involvement of nitrogen and sulphur in metal coordination.

Table 1 Absorption and emission properties of PyTSC and CuPyTSC.

Compound	Absorption	Emission	
	DMF (nm)	DMF (nm)	
		λ_{em} (nm)	ϕ_{em}^a
PyTSC	280,380, 405	440	0.017
[Cu(PyTSC)NO ₃] ₂	280, 365, 380,700	436	0.047

^a ϕ_{em} = emission quantum yield recorded in methanol

The absorption spectra of the compounds (100 μM) were recorded in DMF solvent and the values are summarized in Table 1. The ligand spectrum is dominated by intra-ligand $n \rightarrow \pi^*$ and $\pi \rightarrow \pi^*$ transitions, which are also observed in CuPyTSC. A low energy d-d transition at 700 nm was observed in the spectrum of concentrated solution (1 mM) of the complex (shoulder, Fig. 1A (inset)).

The emission spectra were recorded in DMF solvent (Fig. 1B) by exciting the solution at 370 nm with both excitation and emission slits set at 5. As displayed in the figure, emission peaks of PyTSC ligand and CuPyTSC are observed at 440 and 436 nm respectively and the

absence of the emission when excited at 700 nm of complex suggests ligand-based emission. Further, the complex shows higher emission intensity than PyTSC. This can be attributed to separation of excited states of Cu^{2+} and pyrene via distortion in the geometry.

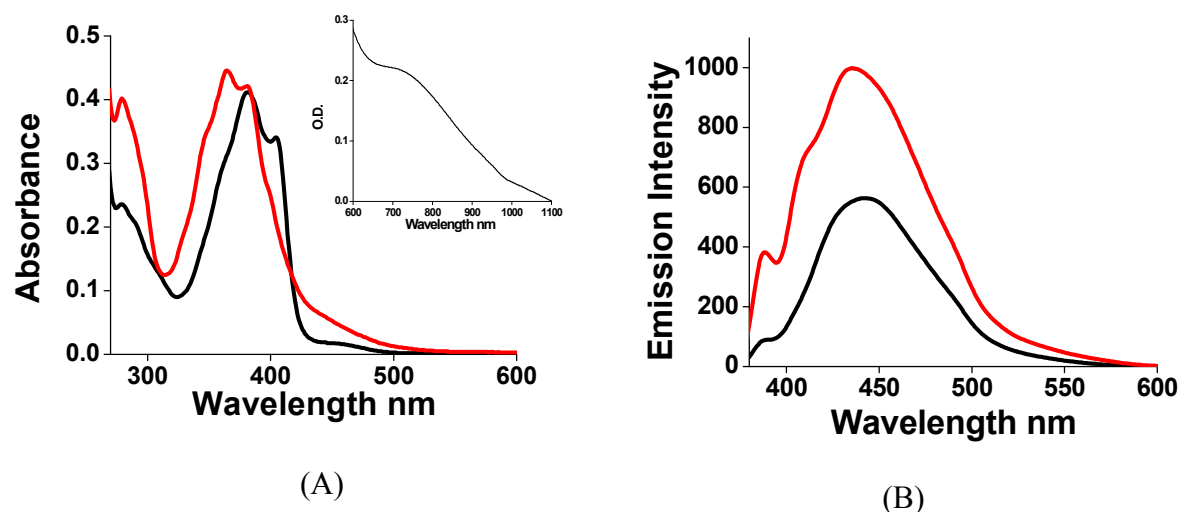


Fig. 1. Absorption (A) and emission spectra (B) of PyTSC (100 μM , black) and CuPyTSC (100 μM , red) in DMF.

The thione-thiol tautomerism of thiosemicarbazone ligands is facilitated in the solution. Therefore, the absorption spectra of ligand were recorded in protic (MeOH, EtOH) and aprotic solvents (CH_3CN , DMF, THF) (Fig. 2A). A red shift of ~ 20 nm was observed in the ligand in aprotic solvents. On the contrary, CuPyTSC at 50 μM concentration show no such effect. The emission spectra (Fig. 2B) of ligand revealed enhanced fluorescence in protic solvents (MeOH, EtOH) contrary to aprotic solvents (CH_3CN , DMF and THF). It may thus be conjectured that hydrogen bonding interactions between ligand and protic solvents inhibit the thione-thiol tautomerism. On the contrary, thiol configuration stabilized by copper in CuPyTSC in aprotic solvent emerge with fluorescence.

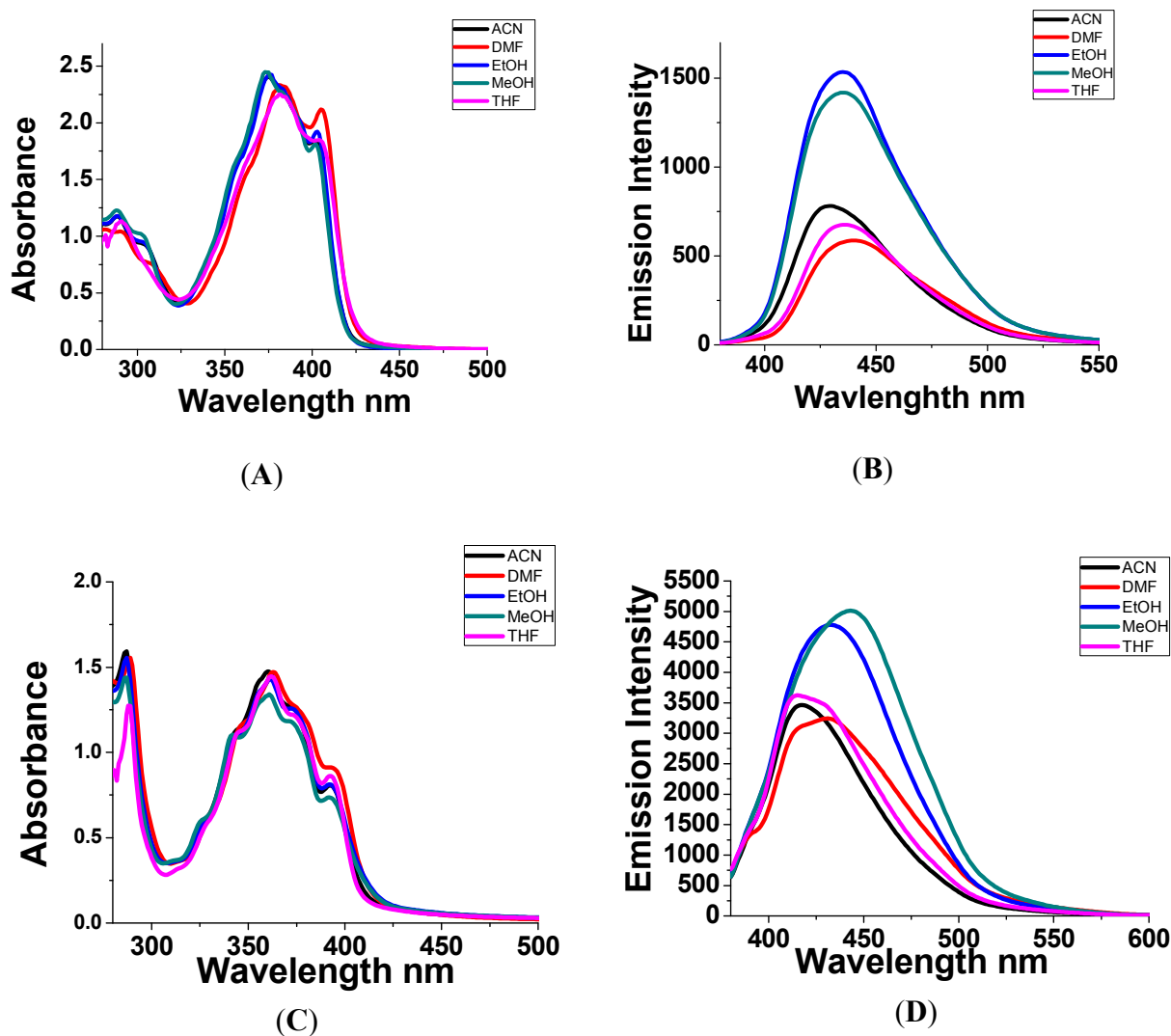


Fig. 2. Effect of solvent polarity on absorption (A) and emission (B) spectra of 50 μ M PyTSC; absorption (C) and emission (D) spectra of 50 μ M CuPyTSC.

3.2 Electrochemical investigations

Electrochemical studies of PyTSC and CuPyTSC have been carried out in dry dimethyl formamide (DMF) and all the potentials were referenced to the standard Ag/AgCl reference electrode. Voltammetric data for PyTSC and CuPyTSC are presented in Table S3 and the cyclic voltammograms are displayed in Fig. 3.

PyTSC exhibited an oxidation peak at 1.23 V vs Ag/AgCl which is assigned to irreversible oxidation of pyrene unit into radical cation.⁹⁷ This process is irreversible due perhaps to either the generation of a dimeric species through association of the oxidized pyrene with a second pyrene subunit or via interaction with the solvent. Cyclic voltammogram of PyTSC exhibits a quasi-reversible peak at -1.95 V which can be assigned to reduction of pyrene to pyrene anion.⁹⁸ Peak to peak separation for this quasi-reversible redox peak was 80 mV, slightly more than that observed for one electron reversible Nernstian process (59 mV). The corresponding peak in pyrene was observed at -2.16 V vs SCE recorded in 1:1 acetonitrile/anhydrous benzene solvent mixture.^{99,100} In addition, three smaller reduction waves observed in PyTSC at -0.37, -0.73 and -1.1 V respectively can be attributed to the formation of other byproducts from subsequent fast chemical reactions. On potential cycling an insoluble film was formed on the working electrode in PyTSC which suggests tendency to form polymeric species⁹⁹ unlike for the copper complex. In CuPyTSC, a peak at 0.75 V is assigned to irreversible oxidation of copper center. A reduction peak centered at 0.098 V further can be assigned to delayed reduction of the oxidized species. Complexation with copper shifted the redox potential of pyrene anion by ~ 0.5 V. It may thus be inferred that coordination of copper reduces the reversibility of the redox system as a result of increased charge transfer from pyrene unit in PyTSC to coordinated copper center. Similar shifts in cobalt complexes are observed in other pyrene derivatives.¹⁰¹

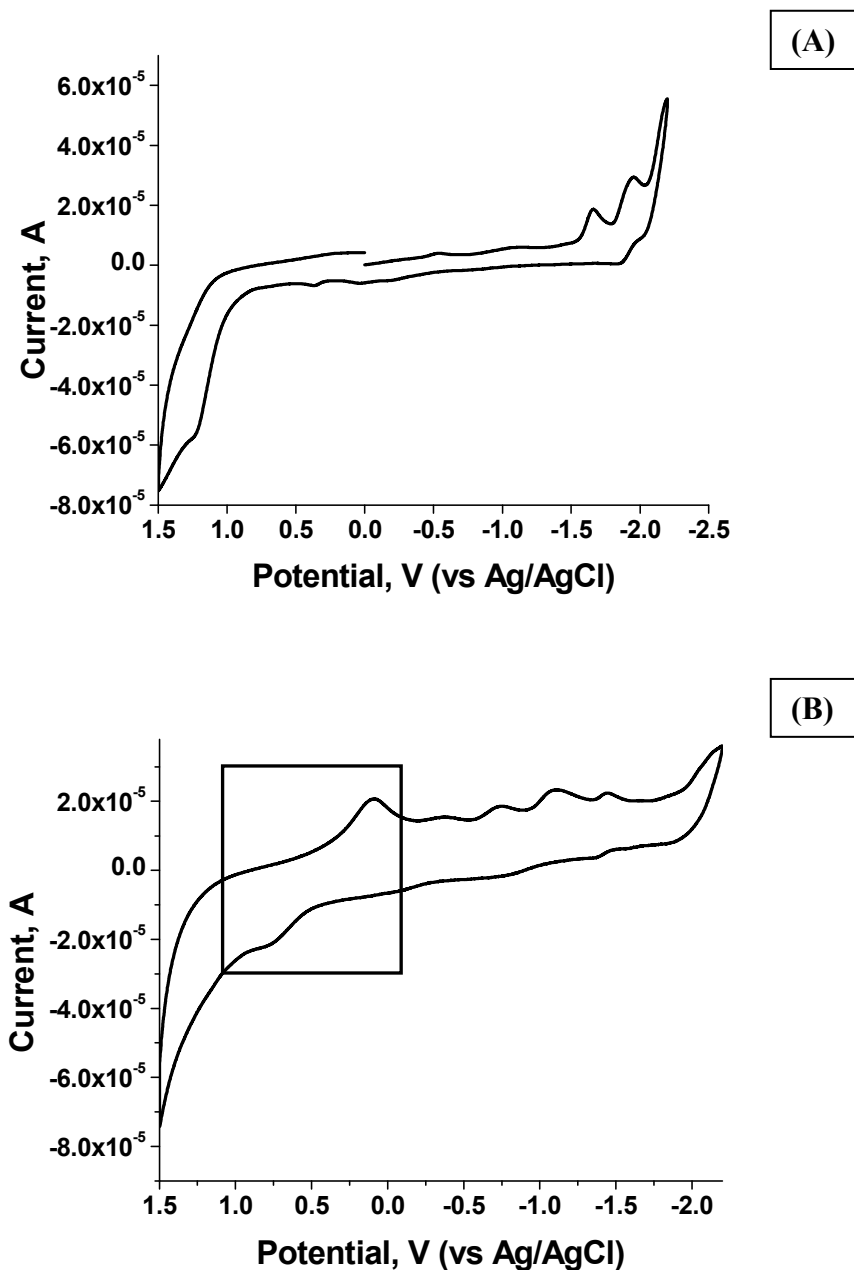


Fig. 3. Cyclic voltammograms of 10^{-3} M solutions of (A) PyTSC and (B) CuPyTSC in DMF solvent using 0.1 M tetrabutylammonium perchlorate as a supporting electrolyte at scan rate 100 mV/s.

3.3 DNA binding studies

DNA is a key target of many antitumor drugs and therefore ability of a drug to bind DNA is often studied by different spectroscopic techniques.¹⁰² Electronic absorption spectroscopy is

the most useful technique for understanding metal complex-DNA interactions. With this perspective absorption spectral titration of PyTSC and CuPyTSC with CT DNA was carried out by monitoring the ligand-based UV transition bands (320-450 nm, Fig. S1). The hypochromism, characteristic of intercalative binding as a result of stacking of planar aromatic pyrene moiety between DNA base pairs¹⁰³ was observed for the ligand as well as the Cu complex. The intrinsic binding constant, K_b , turns out to be of the order of 10^5 for both the compounds.

Table 2 Electronic absorption data upon addition of CT-DNA.

Compound	Hypochromism, H (%)	K_b (M^{-1})
PyTSC	8.5	1.04×10^5
CuPyTSC	14.4	1.20×10^5

3.4 Ethidium Bromide Displacement Assay

EB is a classical intercalator whose fluorescence intensity is enhanced upon complexation with DNA.¹⁰⁴ To ascertain the mode of binding of PyTSC and CuPyTSC to the calf thymus DNA (CT-DNA), a competitive ethidium bromide (EB) displacement assay was performed. Changes in emission intensity of EB bound to CT-DNA were monitored as a function of ligand or complex concentration. A considerable decrease in the fluorescence intensity of the EB-DNA complex upon addition of PyTSC and CuPyTSC was attributed to intercalation of pyrene ring into DNA (Fig. 4). The apparent binding constant (K_{APP}) was calculated using following equation(3)

$$K_{EB}[EB] = K_{APP} [\text{Complex}] \quad (3)$$

Where K_{EB} is $1 \times 10^7 \text{ M}^{-1}$ and the concentration of EB is $10 \text{ } \mu\text{M}$; [complex] is the concentration of the complex causing 50% reduction in the emission intensity of EB. The K_{APP} values for PyTSC and CuPyTSC are 4.0×10^6 and $6.6 \times 10^6 \text{ M}^{-1}$ respectively. The large K_{APP} suggests that these compounds bind to DNA by intercalation.

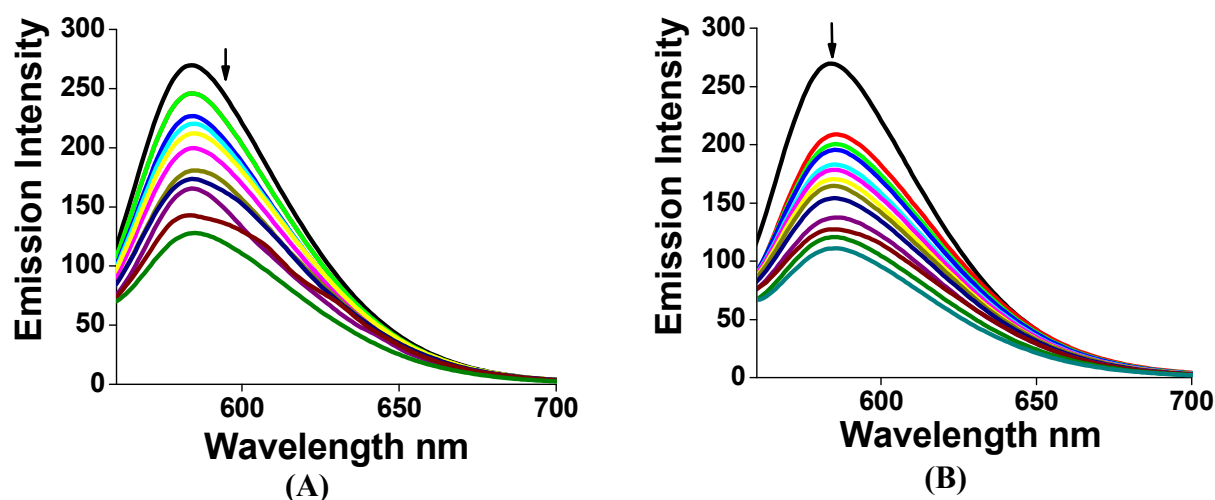


Fig. 4. Effect of addition of (A) PyTSC and (B) CuPyTSC on the emission intensity of the CT-DNA bound ethidium bromide ($10 \text{ } \mu\text{M}$) at different concentrations in 10% DMF- phosphate buffer (pH 7.2).

3.5 Viscosity studies

To verify the interaction of PyTSC and CuPyTSC with DNA, viscosity measurements were carried out in phosphate buffer of pH 7.2. A significant increase in the viscosity of DNA on the addition of complex was observed due to lengthening of DNA helix which is indicative of intercalation.¹⁰⁵ On the other hand, no change in DNA solution viscosity is expected if complex binds in DNA grooves by partial and/or nonclassical intercalation. The effect of increasing concentration of the ligand and complex on the relative specific viscosity of DNA has been displayed in Fig. 5. Increase in viscosity proportional to increasing concentration of PyTSC and CuPyTSC corroborates the earlier inference of intercalation.¹⁰⁶

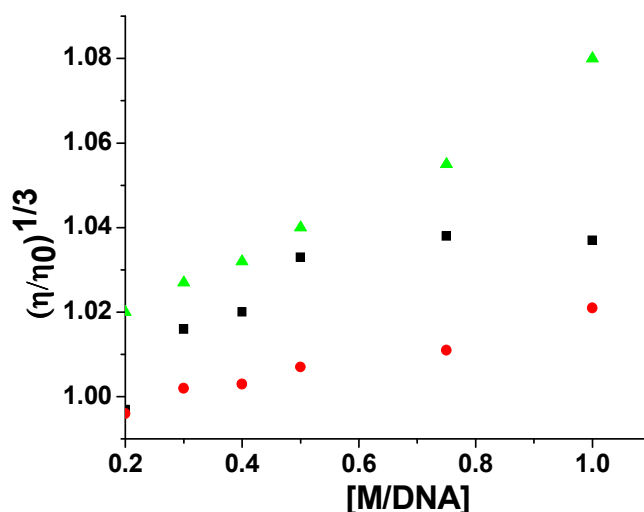


Fig. 5. Effect of increasing amount of PyTSC (■), CuPYTSC (●) and EtBr (▲) on the relative viscosities of calf thymus DNA at 28 °C, [DNA] = 100 μM.

3.6 DNA Cleavage Studies

It is known that DNA cleavage depends on relaxation of supercoiled circular conformation of pBR322 DNA to nicked circular or linear conformations. The fastest migration will be observed for DNA of closed circular conformations (Form II) when potential is applied to circular plasmid DNA. The supercoil relaxes to form a slower moving nicked conformation (form II) if one of the strand is cleaved. The cleavage of both strands leads to a linear conformation (Form III) which migrates between supercoiled and the nicked circular forms.¹⁰⁷⁻¹⁰⁹ Incubation of PyTSC and CuPyTSC with pBR322 DNA in dark shows no cleavage of DNA (Fig. S2). However, photoirradiation of CuPyTSC at 365 nm displays ~74 % DNA cleavage compared to ~14 % in case of PyTSC. Similar observations were made by Chakravarty *et al.* using pyrenyl-terpyridine(py-tpy) lanthanide complexes wherein py-tpy has shown only 15% DNA cleavage compared to its corresponding La(III) complex (88%) on exposure to UV-A light of 365 nm.¹⁰⁷ The better DNA-cleavage ability of the complex was attributed to facile generation of singlet

oxygen species on photoexcitation; however, the reason behind lower DNA-cleavage efficiency of py-tpy was not discussed in details.

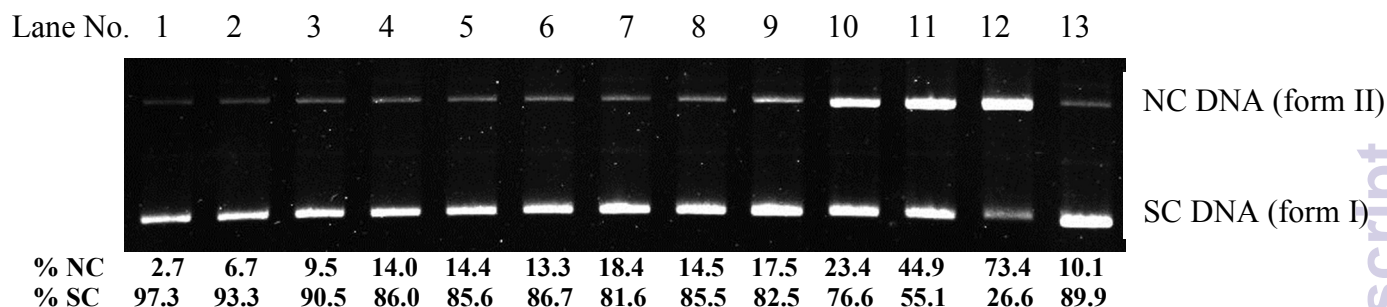


Fig. 6. Photograph of 1% agarose gel showing cleavage of plasmid pBR 322 DNA by PyTSC and CuPyTSC incubated at 37°C for 30 min followed by irradiation for 20 min. [DNA] = 200 ng, Lane 13 DNA control, Lanes 1-6, DNA + 5, 10, 15, 20, 25, 30 μM PyTSC; Lanes 7-12, DNA + 5, 10, 15, 20, 25, 30 μM CuPyTSC

To elucidate how CuPyTSC brings about the DNA cleavage on photoirradiation, 30 μM complex was incubated with different ROS inhibitors. As may readily be noticed from Fig. 7, DMSO, mannitol (hydroxyl radical scavenger) and superoxide dismutase (superoxide radical scavenger) had no effect on DNA cleavage. On the other hand DABCO (lane 3), L-histidine (lane 4) and sodium azide (lane 5), all singlet oxygen scavengers, were able to inhibit cleavage of plasmid DNA induced by CuPyTSC, indicating involvement of singlet oxygen. It has been reported that non-porphyrinic Cu(II) complexes can cause significant DNA cleavage in presence of suitable photosensitizers in ternary system through singlet oxygen generation.⁷⁴ Since PyTSC is a conjugate of two photosensitizers, viz. TSC and pyrene, we expected more efficient generation of singlet oxygen causing more DNA cleavage on photoexposure. Therefore, to investigate the photosensitization proficiency of PyTSC and its Cu(II) complex, we performed DFT calculations.

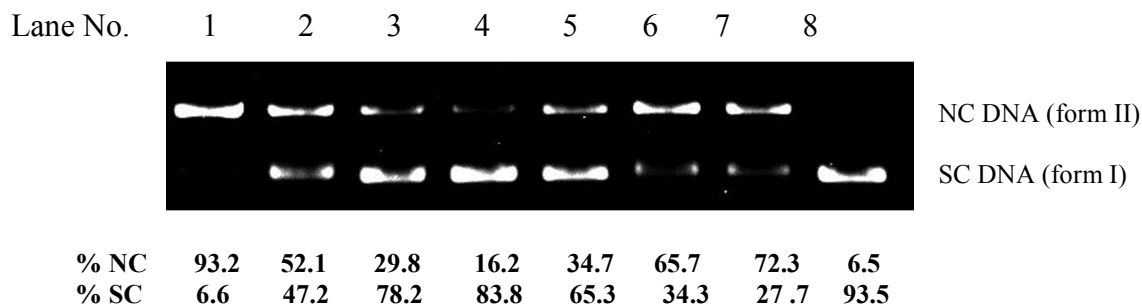


Fig. 7. Photograph of 1% agarose gel showing the effect of inhibitors on cleavage of pBR322 plasmid DNA by CuPyTSC [DNA] =300 ng, CuPyTSC = 30 μ M, Lane 8 = DNA control; lane 7 = DNA + CuPyTSC; lane 1 = DNA + CuPyTSC+ DMSO; lane 2 = DNA + CuPyTSC + mannitol (50 mM); lane 3 = DNA + CuPyTSC + DABCO (10 mM); lane 4 = DNA + CuPyTSC + L-histidine (20 mM); lane 5 = DNA + CuPyTSC + NaN_3 ; (20 mM) lane 6 = DNA + CuPyTSC + SOD (15 units). Inhibitors were added to DNA solution prior to addition of CuPyTSC, incubated for 30 min and then irradiated for 20 min.

3.7 Theoretical Study

Optimized structures of Py, TSC, PyTSC and CuPyTSC from the B3LYP/6-31g(d,p) theory are depicted in Fig. 8 along with selected bond distances and bond angles. As shown in Figure, the CuPyTSC comprises of two Cu^{2+} ions showing locally distorted tetrahedral structures bridged through ONO linkages. Cu^{2+} and one of the PyTSC units orient mutually at an angle of 132° ($d(\text{O}-\text{Cu}-\text{N}2-\text{N}3)$) while other PyTSC moiety shows a deviation of 84° from planarity. This deviation does not bring about effective overlap of $\pi\pi^*$ orbitals of PyTSC with those of Cu^{2+} which in turn inhibits communication between copper(II) and excited states of pyrene on absorption of light. The excited pyrene then comes to ground state by giving fluorescence and Cu^{2+} decays via non-radiative pathway leading to high emission of CuPyTSC. In this regard it may be worth noting that the investigations on pyrene functionalized bis(thiosemicarbazonato) copper(II) complexes carried out by Holland and coworkers employing the single photon emission experiments combined with the density functional theoretic calculations led to similar inferences.⁸⁴

Highest occupied molecular orbital (HOMO) and lowest unoccupied molecular orbital (LUMO) in Py, TSC, PyTSC shown in Fig. S6 of the supporting information reveal the electron-rich regions in these systems by and large, reside on aromatic moieties and the S centre. The charge distribution in CuPyTSC is portrayed in Fig. 9 displaying localized HOMO near one of the PyTSC moieties. A charge transfer from one PyTSC moiety to the other one in the CuPyTSC is further evident from the complementarity of electron-rich regions in the HOMO and LUMO. The present calculations have shown the emergent hierarchy for the separation of HOMO-LUMO energies (in eV) viz., Py (0.984) > TSC (0.739) > PyTSC (0.629) > CuPyTSC (0.332) which predicts greater photosensitization ability for CuPyTSC than PyTSC as a result of increased production of singlet oxygen bringing about DNA-cleavage.

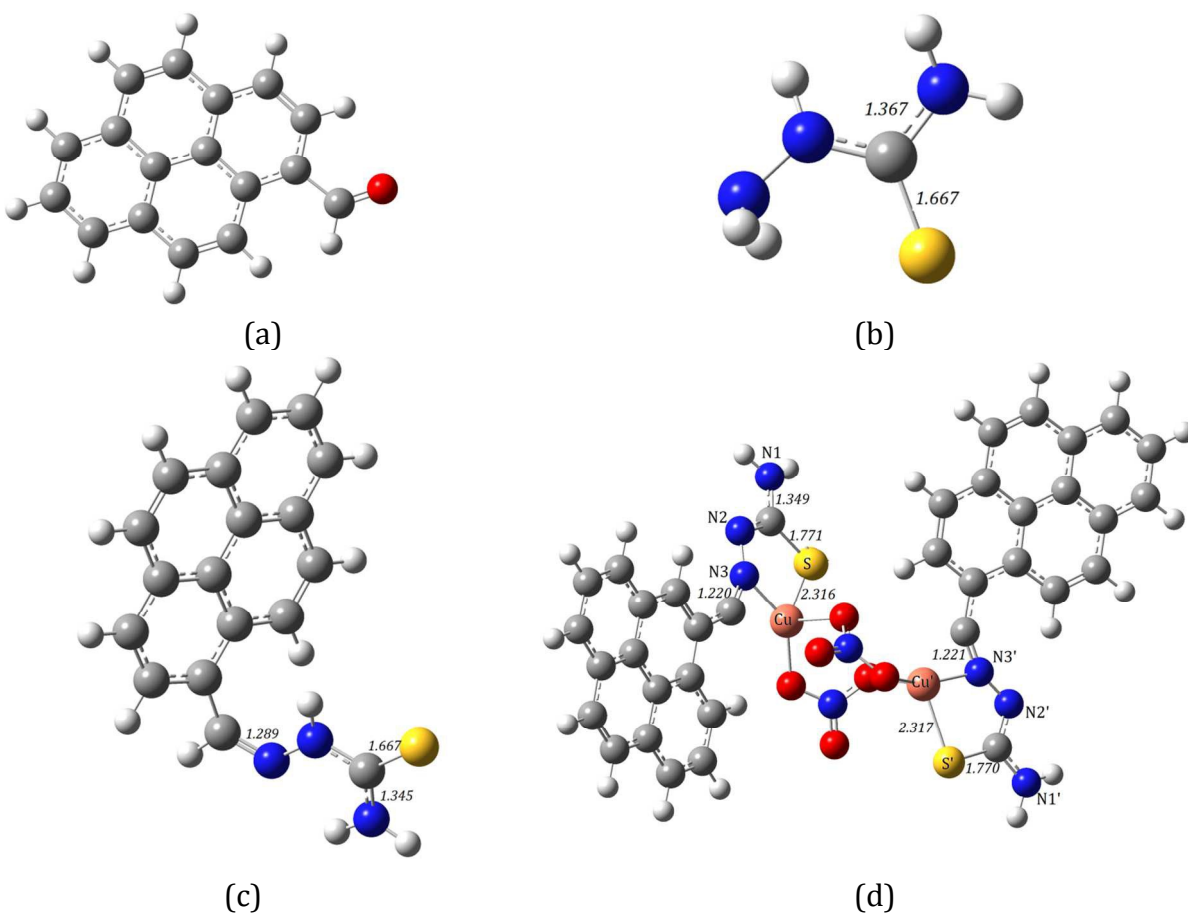


Fig.8: B3LYP/6-31G (d,p) optimized geometries of (a) Py, (b) TSC, (c) PyTSC and (d) CuPyTSC. Selected bond distances (in Å) are given alongwith.

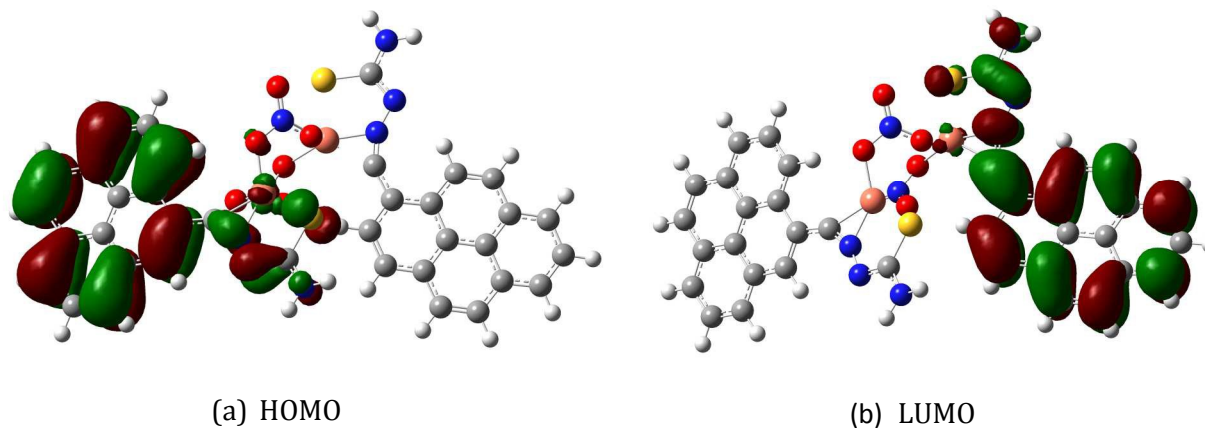


Fig. 9. HOMO and LUMO (isosurfaces of 0.02 a.u) (a) 1-pyrenecarboxaldehyde and (b) 1-pyrenecarboxaldehyde thiosemicarbazone of CuPyTSC.

3.8 Protein Binding

Serum albumins are the most extensively studied proteins because of their stability and unusual ligand binding properties. In addition, albumin is the most important transport protein and plays a significant role in the transport and deposition of a variety of substances in blood.¹¹⁰ Understanding the binding of drug to protein yield insights accompanying drug metabolism and transport and further establish protein structure-function relationship. Therefore, bovine serum albumin (BSA) has been studied extensively in the past due to its structural homology with human serum albumin.¹¹¹⁻¹¹³ The protein-bound complexes are transported through biological fluids and released at cellular level to exhibit anticancer activity by inhibiting certain fundamental enzyme function(s) and can give insights into the mechanism of action.¹¹⁴ Palaniandavar *et al.* have demonstrated that one of the Cu(II) complexes, $[\text{Cu}(\text{pmdt})(5,6\text{-dmp})]^{2+}$, where pm dt is N,N,N',N'',N'''-pentamethyldiethylene triamine and 5,6-dmp is 5,6-dimethylphenanthroline, exhibit highest affinity to DNA and BSA and thus acts as a promising antitumor agent.¹¹³ The apotransferrin-bound anticancer drug KP1019 (i.e., indazolium *trans-*

[tetrachlorobis(*1H*-imidazole)ruthenate(III))] gets transported via transferrin cycle and exhibits a higher antitumor activity than the intact complex alone.¹¹⁵ Another Ru(II) anticancer compound, (H₂im) *trans*-[RuCl₄(DMSO)(Him)] where Him = imidazole (NAMI-A), undergoing human trials, forms adduct with BSA. The kinetics and mechanism of adduct formation is proposed to influence its anticancer activity.¹¹⁶ For this reason, we have carried out protein binding studies of PyTSC and CuPyTSC to understand the extent of binding and its effect on cytotoxicity profile of the compounds.

Tryptophan emission-quenching experiments were carried out using BSA in the presence of PyTSC and CuPyTSC. The BSA solution shows a strong emission peak at 340 nm ($\lambda_{\text{ex}} = 285$ nm) due to tryptophan residues. Emission intensity of BSA solution is controlled by various factors such as the degree of exposure of tryptophan residues, polar solvent and presence of specific quenching groups.¹¹⁷⁻¹¹⁹ Addition of PyTSC and CuPyTSC to BSA resulted in significant emission quenching at 340 nm as portrayed in Fig. 10. The fluorescence at 340 nm was corrected for the inner filter effect, according to equation (4)¹²⁰

$$F_{\text{corr}} = F_{\text{obs}} \cdot 10^{A_{\text{exc}}/2} \quad (4)$$

where F_{corr} is the corrected fluorescence intensity, F_{obs} is the observed fluorescence intensity at 340 nm. A_{exc} is absorbance at 285 nm. The corrected fluorescence intensity data was then analyzed using Stern–Volmer equation:

$$F_0/F = 1 + K_{\text{SV}}[Q] = 1 + k_q\tau_0[Q] \quad (5)$$

where F_0 and F are the fluorescence intensities at 340 nm in the absence and presence of quencher, respectively, τ_0 denotes the lifetime of the fluorophore in the absence of quencher, $[Q]$ is the quencher concentration, K_{SV} is the Stern–Volmer quenching constant, and k_q , the bimolecular quenching rate constant.

Stern–Volmer quenching constants for PyTSC and CuPyTSC obtained by linear regression of SV plots, were found to be 1.37×10^3 and 2.69×10^3 L mol⁻¹, respectively at 28°C. For BSA, τ_0 is known to be approximately 1×10^{-8} s and accordingly the quenching rate constant, k_q , turns out to be 1.37×10^{11} and 2.69×10^{11} mol⁻¹s⁻¹, respectively for PyTSC and CuPyTSC.

The number of binding sites were obtained from :

$$\text{Log } (F_0 - F / F) = \text{log } K_A + n \text{ log } [Q] \quad (6)$$

Where K_A is the association constant and n = number of binding sites. The association constants for PyTSC and CuPyTSC were found to be 1.92×10^4 and 2.52×10^4 M⁻¹ respectively suggesting moderate binding to BSA. The number of binding sites as obtained from slope of the double-log plots (Fig. S7) for PyTSC and CuPyTSC on BSA are 1.3 and 2.4 respectively. The binding ratio of PyTSC to BSA was observed to be 1:1 and two molecules of CuPyTSC are interacting with one BSA molecule. All correlation coefficients are about 0.99, indicating that the interaction between PyTSC and CuPyTSC with BSA are consistent with the site-binding model. Differences in relative binding strengths can be attributed to the hydrogen bonding and π -stacking interactions with appropriate stereochemical arrangement of the compounds.

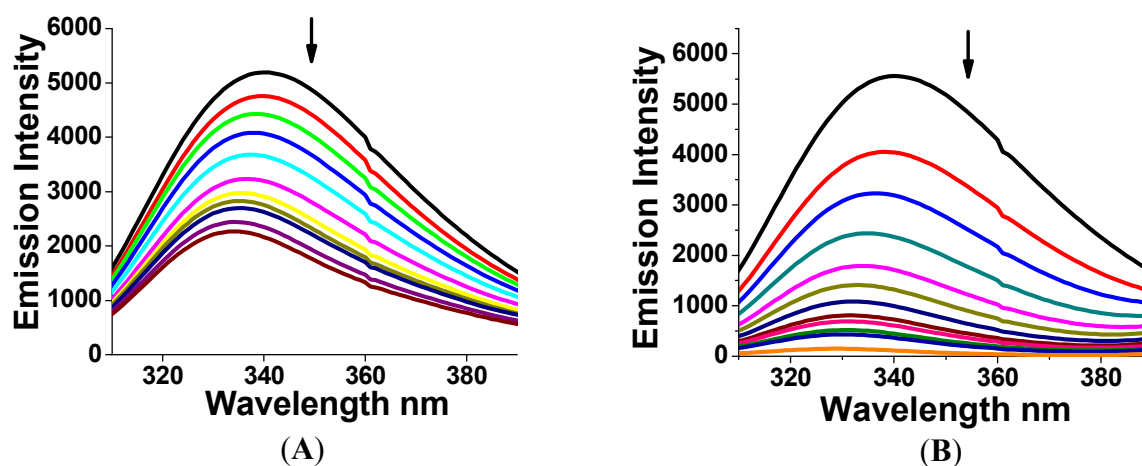


Fig. 10. Effect of addition of (A) PyTSC and (B) CuPyTSC on the emission intensity of the BSA (50 μM) at different concentrations in 10% DMF phosphate buffer (pH 7.2).

3.9 Cellular uptake and Cell Cytotoxicity Studies:

The uptake of PyTSC and CuPyTSC by cancer cells was monitored by fluorescence microscopy. Bright green fluorescence was observed (Fig. 11) when cells (B16F10, melanoma cell line) were incubated with 30 μM concentrations of PyTSC and CuPyTSC for 8 h at 37 $^{\circ}\text{C}$ in 5% CO_2 incubator indicating that the compounds are taken up by the cells. It has been noted that, at 30 μM concentration, whole cytoplasm was stained in contrast to enhanced accumulation in nucleus on photoexposure. The effect of radiation was also tested on control cells. No appreciable change in the cell viability was observed in the cells incubated in dark (Fig. 11 (a)) and the ones photoexposed for 30 min (Fig.11 (d)) before incubation suggesting that the effect observed is due to the compounds alone. Careful observations of the images (e) and (f) reveal cytoplasmic vacuolization on exposure to monochromatic light of 365 nm suggesting a different mode of action of these compounds in dark and on photoirradiation.

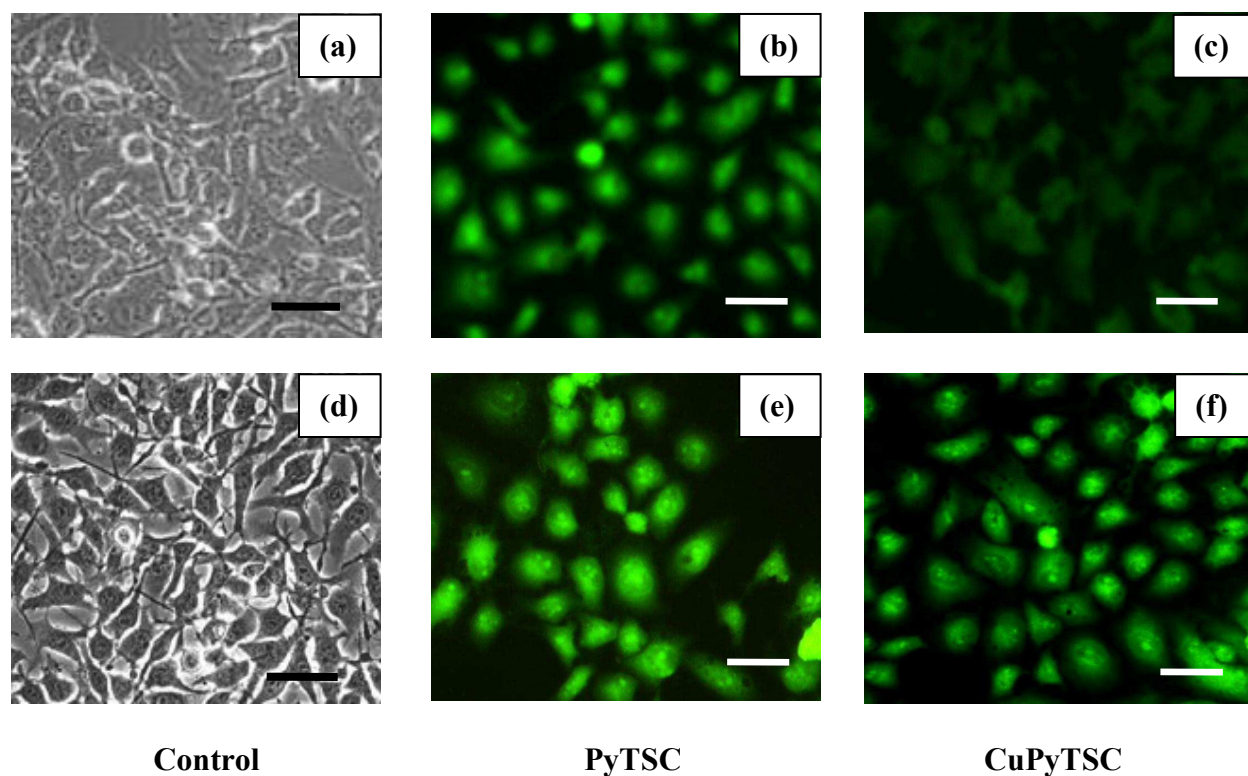


Fig. 11. Fluorescence microscopic images of B16F10 melanoma cells indicating cellular uptake of PyTSC and CuPyTSC (30 μM) after 8 h with treatments as indicated; UV specifies exposure to 365 nm light for 30 min prior to incubation. (a) Untreated cells (control, dark), (b) PyTSC, (c) CuPyTSC (d) Untreated cells (control, UV), (e) PyTSC (UV), (f) CuPyTSC (UV). Scale bar = 20 μm .

Fig. 12 shows the result of cell cytotoxicity on B16F10 melanoma cells using MTT assay. The cells were treated with different concentrations of PyTSC and its copper complex for 24 h. When incubated in dark, PyTSC showed higher cytotoxicity than CuPyTSC. However, on 30 min exposure to UV light of 365 nm, no appreciable increase in the toxicity of PyTSC was observed. On the other hand, exposure to 365 nm light nearly doubled the cell death by CuPyTSC (~90%) at 50 μM concentration. This can be attributed to the facile singlet oxygen generation by CuPyTSC on exposure to UV light through photosensitization (vide sections 3.6 and 3.7), bringing about more cell death. Further, variation in the cytotoxicity profiles of the ligand and

its copper complex indicate the differences in their cellular uptake and processing. Detailed studies to investigate the mechanism of action are currently underway.

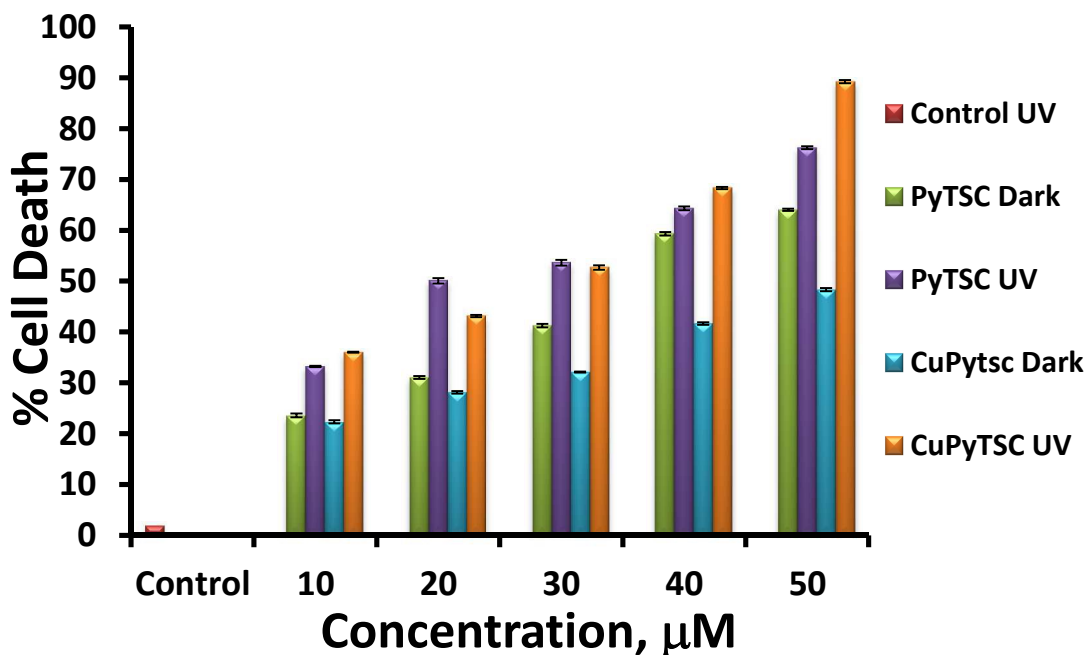


Fig. 12. Effect of concentration on viability of B16F10 melanoma cells as determined by MTT assay. Dark means the test compounds were incubated with cells in dark, while UV indicate the test compounds exposed to UV light of 365 nm for 30 min, then further incubated upto 24 h in dark. Control represents cells exposed to 365 nm light for 30 min without PyTSC and CuPyTSC. The error bars indicate standard deviation from experiments performed in triplicate.

4. Conclusions

Our results demonstrated that PyTSC on binding to Cu(II) yielded a highly fluorescent complex. Both, ligand and complex, bind to CT-DNA via intercalation with binding constants of the order of 10^5 . The compounds did not show any appreciable cleavage of plasmid pBR322 DNA when incubated in dark. On photoirradiation, CuPyTSC displayed greater DNA cleavage (74%) ability than PyTSC (14%). Mechanistic investigations revealed involvement of singlet oxygen species in the DNA cleavage by both the compounds. DFT calculations evidenced a

decreased HOMO-LUMO gap for CuPyTSC (0.332 eV) as compared to PyTSC (0.629 eV) which can be correlated to better photosensitization ability of the complex. From DFT calculations, high emission intensity of CuPyTSC was found to be due to poor overlap of π - π^* orbitals consequent to twisting of PyTSC bound to Cu(II), which separated the excited states of Cu^{2+} from pyrene. The Cu^{2+} excited state was speculated to be decaying faster nonradiatively whereas pyrene decays with high emission intensity. Both the compounds bind to bovine serum albumin with moderate binding constant of 10^4 suggesting formation of ground state complex between BSA and compounds. PyTSC and CuPyTSC were taken up by the B16F10 (melanoma) cells and give green fluorescence when observed under fluorescence microscope. These compounds lead to no considerable cell death when incubated in dark; however, CuPyTSC induces more cell death on exposure to UV light than ligand alone. Thus, better DNA and protein binding affinity coupled with greater oxidative DNA cleavage by CuPyTSC is consistent with its higher cytotoxicity.

Acknowledgments:

ANK acknowledges financial support from D. B. Limaye Trust. SSR is thankful to University of Pune for the award of research fellowship through the University of Potential excellence scheme from the University Grants commission, New Delhi, India.

Electronic Supplementary Information Available : ESI mass spectra of compounds, images for agarose gel electrophoresis showing DNA cleavage in dark, images of absorption titration of compounds with CT-DNA, Frontier orbitals in (a) TSC, (b) Py and (c) PyTSC (isovalue of ± 0.54 eV), Double-log plots for BSA-PyTSC and BSA-CuPyTSC interactions to calculate

association constant and number of binding sites, tables for selected bond- distances (in Å) and - angles (in °), selected vibrational frequencies of 1-pyrenecarboxaldehyde and 1-pyrenecarboxaldehyde thiosemicarbazone optimized at wB97x/6-31G (d, p) and electrochemical data of PyTSC and CuPyTSC are available at www.pubs.rsc.org.

References

1. Z. Guo and, P. J. Sadler, *Angew. Chem. Int. Ed.*, 1999, **38**, 1512-1531.
2. M. J. Abrams and B. A. Murrer, *Science*, 1993, **261**, 725-730.
3. D. H. Lee, T. R. O'connor and G.P. Pfeifer, *Nucl. Acid. Res.*, 2002, **30**, 3566-3573.
4. M. A. Cater, H. B. Pearson, K. Wolyniec, P. Klaver, M. Bilandzic, B. M. Paterson, A. I. Bush, P. O. Humbert, L. S. Fontaine, P. S. Donnelly and H. Haupt, *ACS chem. biol.*, 2013, **8**, 1621-1631.
5. V. Opletalova, D. S. Kalinowski, M. Vejsova, J. Kunes, M. Pour, J. Jampilek, V. Buchta and D. R. Richardson, *Chem. Res. Toxicol.*, 2008, **21**, 1878–1889.
6. H. Beraldo and D. Gambino, *Mini-Rev. Med. Chem.*, 2004, **4**, 31-39.
7. P. F. Salas, C. Herrmann and C. Orvig, *Chem. Rev.*, 2013, **113**, 3450–3492.
8. T. S. Lobana, R. Sharma, G. Bawa and S. Khanna, *Coord. Chem. Rev.*, 2009, **253**, 977-1055.
9. T. S. Lobana, G. Bawa, G. Hundal and M. Zellr, *Anorg. Allg. Chem.*, 2008, 634, 931-937.
10. T. S. Lobana, G. Bawa, A. Castineiras, R. J. Butcher and M. Zeller, *Organometallics*, 2008, **27**, 175-180.
11. T. S. Lobana, Rekha, R. J. Butcher, A. Castineiras, E. Bermejo and P. V. Bharatam, *Inorg. Chem.*, 2006, **45**, 1535-1542.
12. T. S. Lobana S. Khanna, G. Hundal, P. Kaur, B. Thakur, S. Attri and R. J. Butcher,

- Polyhedron*, 2009, **28**,1583-1593.
13. T. S. Lobana, S. Khanna, and R. J. Butcher, *Inorg. Chem. Comm.*, 2008, **11**, 11-14.
14. E. W. Ainscough, A. M. Brodie, J. D. Ranford, J. M. Waters and K. S. Murray, *Inorg. Chim. Acta*, 1992,**197**, 107-115.
15. J. Garcia-Tojal, M. K. Urriaga, R. Cortes, L. Lezama, T. Rojo and M. I. Arriortua, *J. Chem. Soc. Dalton Trans.*, 1994, 2233-2238.
16. C. F. Bell and C. R. Theochars, *Acta Crystallogr. Sect. C.*, 1987, **43**, 26-29.
17. A. G. Bingham, H. Bogge, A. Muller, E. W. Ainscough and A. M. Brodie, *J. Chem. Soc. Dalton Trans.*, 1987, 493-499.
18. J. Garcia-Tojal, L. Lezama, J. L. Pizarro, M. Insausti, M. I. Arriortua and T. Rojo, *Polyhedron*, 1999, **18**, 3703-3711.
19. E. W. Ainscough, A. M. Brodie, J. D. Ranford and J. M. Waters, *J. Chem. Soc. Dalton Trans.*, 1997, 1251-1256.
20. J. Garcia-Tojal, J. Grcia-Jaca, R. Cortes, T. Rojo, M. K. Urriaga and M. I. Arrortua, *Inorg. Chim. Acta*, 1996, **249**, 25-32.
21. E. W. Ainscough, A. M. Brodie, J. D. Ranford and J. M. Waters, *J. Chem. Soc. Dalton Trans.*, 1991, 2125-2131.
22. P. Kalaiivani, R. Prabhakaran, F. Dallemer, P. Poornima, E. Vaishnavi, E. Ramachandran, V. Vijaya Padma, R. Renganathan and K. Natarajan, *Metallomics*, 2012, **4**, 101-113.
23. C. Santini, M. Pelli, V. Gandin, M. Porchia, F. Tisato and C. Marzano, *Chem. Rev.*, 2014, **114**, 815-862.
24. A. N. Kate, A. A. Kumbhar, A. A. Khan, P.V. Joshi and V. G. Puranik, *Bioconjugate Chem.* 2014, **25**, 102-114.

25. D. S. Raja, N. S. P. Bhuvanesh and K. Natarajan, *Inorg. Chem.*, 2011, **50**, 12852-12866.
26. D. S. Raja, G. Paramaguru, N. S. P. Bhuvanesh, J. H. Reibenspies, R. Renganathan and K. Natarajan, *Dalton Trans.*, 2011, **40**, 4548-4559.
27. D. X. West, I. H. Hall, K. G. Rajendran and A. E. Liberta, *Anticancer Drugs*, 1993, **4**, 231-240.
28. A. I. Matesanz, C. Joie and P. Souza, *Dalton Trans.*, 2010, **39**, 7059-7065.
29. S. Padhye, Z. Afransiabi, E. Sinn, J. Fok, K. Mehta and N. Rath, *Inorg. Chem.*, 2005, **44**, 1154-1156.
30. T. Wang and Z. Guo, *Curr. Med. Chem.*, 2006, **13**, 525-537.
31. A. Gaál, G. Orgován, Z. Polgári, A. Réti, V. G. Mihucz, S. Bősze, N. Szoboszlai and C. streli, *J. Inorg. Biochem.*, 2014, **130**, 52-58.
32. T. Rosu, E. Pahontu, S. Pasculescu, R. Georgescu, N. Stanica, A. Curaj, A. Popescu and M. Leabu, *Eur. J. Med. Chem.*, 2010, **45**, 1627-1634.
33. D. Palanimuthu, S. V. Shinde, K. Somasundaram and A. G. Samuelson, *J. Med. Chem.*, 2013, **56**, 722-734.
34. D. S. Raja, N. S. P. Bhuvanesh and K. Natarajan, *Eur. J. Med. Chem.*, 2011, **46**, 4584-4594.
35. M. Colberg, K. R. Strand, P. Graff and K. K. Andersson, *Biochim. Biophys. Acta*, 2004, **1699**, 1-34.
36. E. C. Moore, M. S. Zedeck, K. C. Agarwal and A. C. Sartorelli, *Biochemistry*, 1970, **9**, 4492-4498.
37. F. A. French, E. J. Blanz, S. C. Shaddix and R. W. Brockman, *J. Med. Chem.*, 1974, **17**, 172-181.
38. C. R. Cowol, R. Berger, R. Eichinger, A. Roller, M.A. Jakupec, P.P. Schmidt, V. B. Arion,

- and B. K. Keppler, *J. Med. Chem.*, 2007, **50**, 1254-1265.
39. J. P. Holland P. J. Barnard, D. Collison, J. R. Dillworth, R. Edge, J. C. Green and E. J. L. McInnes, *Chem.-Eur. J.*, 2008, **14**, 5890-5907.
40. J. L. J. Dearling, J. S. Lewis, G. E. D. Mullen, M. J. Welch and P. J. Blower, *J. Biol. Inorg. Chem.*, 2002, **7**, 249–259.
41. J. L. J. Dearling, J. S. Lewis, D. W. McCarthy, M. J. Welch and P. J. Blower, *Chem. Comm.*, 1998, 2531-2532.
42. F. A. French and B. L. Freedlander, *Cancer Res.*, 1958, **18**, 1290-1300.
43. H. G. Petering, H. H. Buskirk and G. E. Underwood, *Cancer Res.*, 1964, **24**, 367-372.
44. P. Wolohan, J. Yoo, M. J Welch and D. E. Reichert, *J. Med. Chem.*, 2005, **48**, 5561-5569.
45. M. A. Green, *Int. J. Rad. Appl. Instrum. B.*, 1987, **14**, 59-61.
46. B. M. Paterson and P. S. Donnelly, *Chem Soc. Rev.*, 2011, **40**, 3005-3018.
47. P. D. Bonniticha, A. L. Vavere, J. S. Lewis and J. R. Dilworth, *J. Med. Chem.*, 2011, **51**, 2985-2991.
48. P. S. Donnelly, J. R. Liddell, S. Lim, B. M Paterson, M. A. Cater, M. S. Savva, A. I. Mot, J. L. James, I. A. Trounce, A. R. White and P. J. Crouch, *Proc. Natl. Acad.Sci. U.S.A.*, 2012, **109**, 47-52.
49. N. Adonai, K. N. Nguyen, J. Walsh, M. Iyer, T. Toyokuni, M. E. Phelps, T. McCarthy, D. W. McCarthy, and S. S. Gambhir, *Proc. Natl. Acad. Sci. U.S.A.*, 2002, **99**, 3030-3035.
50. M. A. Green, D. L. Klippenstein and J. R. Tennison, *J. Nucl. Med.*, 1988, **29**, 1549-1557.
51. J. R. Dilworth and R. Hueting, *Inorg. Chim. Acta*, 2012, **389**, 3-15.
52. O. Baudoin, M.-P. Teulade-Fichou, J.-P. Vigneron and J.-M. Lehn, *Chem. Commun.*, 1998

2349-2350.

53. M. Gonzalez-Alvarez, G. Alzuet, J. Borrás, M. Pitie and B. Meunier, *J. Biol. Inorg. Chem.*, 2003, **8**, 644-652.
54. J. H Kim and S. H. Kim, *Chem. Lett.*, 2003, **32**, 490- 491.
55. A. Garca-Raso, J.J. Fiol, B. Adrover, V. Moreno, I. Mata, E. Espinosa and E. Molins, *J. Inorg. Biochem.*, 2003, **95**, 77- 86.
56. L.-P. Lu, M.-L. Zhu and P. Yang, *J. Inorg. Biochem.*, 2003, **95**, 31- 36.
57. A. Patwardhan and J. A. Cowan, *Chem. Commun.*, 2001, 1490-1491.
58. D. S. Sigman, *Biochemistry*, 1990, **29**, 9097 - 9105.
59. T. B. Thederahn, M. D. Kuwabara, T. A. Larsen and D. S. Sigman, *J. Am. Chem. Soc.*, 1989, **111**, 4941- 4946.
60. O. Zelenko, J. Gallagher and D. S. Sigman, *Angew. Chem., Int. Ed. Engl.* 1997, **36**, 2776- 2778.
61. M. M. Meijler, O. Zelenko and D. S. Sigman, *J. Am. Chem. Soc.* 1997, **119**, 1135- 1136.
62. E. L. Hegg and J. N. Burstyn, *Coord. Chem. Rev.* 1998, **173**, 133- 165.
63. D. K. Chand, H.-J. Schneider, A. Bencini, A. Bianchi, C. Giorgi, S. Ciattini and B. Valtancoli, *Chem. Eur. J.*, 2000, **6**, 4001- 4008.
64. R. Hettich, H.-J. Schneider, *J. Am. Chem. Soc.* 1997, **119**, 5638- 5647.
65. J. A. Cowan, *Chem. Rev.* 1998, **98**, 1067- 1088.
66. F. H. Westheimer, *Science* 1987, **235**, 1173- 1178.
67. D. E. Wilcox, *Chem. Rev.* 1996, **96**, 2435- 2458.
68. M. Komiyama and J. Sumaoka, *Curr. Opin. Chem. Biol.* 1998, **2**, 751-757.
69. H. J. Eppley, S. M. Lato, A. D. Ellington and J. M. Zaleski, *Chem. Commun.*, 1999, 2405-

- 2406.
70. S. Dhar and A.R. Chakravarty, *Inorg. Chem.* 2003, **42**, 2483-2485.
71. A. K. Patra, S. Dhar, M. Nethaji and A. R. Chakravarty, *Chem. Commun.*, 2003, 1562-1563.
72. S. Dhar, D. Senapati, P. K. Das, P. Chattopadhyay, M. Nethaji and A.R. Chakravarty, *J. Am. Chem. Soc.* 2003, **125**, 12118- 12124.
73. S. Dhar, D. Senapati, P. A. N. Reddy, P. K. Das and A. R. Chakravarty, *Chem. Commun.*, 2003, 2452-2453.
74. A. M. Thomas, A. D. Naik, M. Nethaji and A. R. Chakravarty, *Inorg. Chim. Acta*, 2004, **357**, 2315–2323.
75. C. Molenaar, J. M. Teuben, R. J. Heetebrij, H. J. Tanke and J. Reedijk, *J. Biol. Inorg. Chem.* 2000, **5**, 655-665.
76. E. J. New, R. Duan, J. Z. Zhang and T. W. Hambley, *Dalton Trans.*, 2009, 3092-3101.
77. S. Lim, K. A. Price, S. F. Chong, B. M. Paterson, A. Caragounis, K. J. Barnham, P. J. Crouch, J. M. Peach, J. R. Dilworth, A. R. White and P. S. Donnelly, *J. Biol. Inorg. Chem.*, 2010, **15**, 225-235.
78. S. I. Pascu, P. A. Waghorn, B. W. C. Kennedy, R. Arrowsmith, S. R. Bayly, J. R. Dilworth, M. Christlieb, R. M. Tyrrell, J. Zhong, R. M. Kowalczyk, D. Collison, P. K. Aley, G. C. Churchill, F. I. Aigbirhio, *Chem. Asian J.*, 2010, **5**, 506-519.
79. S. I. Pascu, P. A. Waghorn, T. D. Conry, B. Lin, H. M. Betts, J. R. Dilworth, R. B. Sim, G. C. Churchill, F. I. Aigbirhio, J. E. Warren, *Dalton Trans.*, 2008, 2107-2110.
80. S. I. Pascu, P. A. Waghorn, T. D. Conry, H. M. Betts, J. R. Dilworth, G. C. Churchill, T. Pokrovskaya, M. Christlieb, F. I. Aigbirhio and J. E. Warren, *Dalton Trans.*, 2007, 4988-4997.
81. M. Christlieb, A. R. Cowley, J. R. Dilworth, P. S. Donnelly, B. M. Paterson, H. S. R.

- Struthers and J. M. white, *Dalton Trans.*, 2007, 327-331.
82. R. L. Arrowsmith, P. A. Waghorn, M. W. Jones, A. Bauman, S. K. Brayshaw, Z. Hu, G. Kociok-Kohn, T. L. Mindt, R. M. Tyrrell, S. W. Botchway, J. R. Dilworth and S. I. Pascu, *Dalton Trans.*, 2011, **40**, 6238-6252.
83. M. Christlieb and J. R. Dilworth, *Chem. Eur. J.*, 2006, **12**, 6194-6206 and references therein.
84. J. P. Holland, V. Fisher, J. A. Hickin and J. M. Peach, *Eur. J. Inorg. Chem.*, 2010, 48-58.
85. Q. Xuhong, H. Tian-Bao, W. Dong-Zhi, Z. Dong-Hui, F. Mingcai, Y. Wei, *J. Chem. Soc., Perkin Trans. 2*, 2000, 715- 718.
86. A. Jakobs and J. Piette, *J. Med. Chem.*, 1995, **38**, 869- 874.
87. S. Murov, I. Carmichael and G. L. Hugin, *Handbook of Photochemistry*, 2nd Edn, Marcel Dekker, New York, 1993
88. J. Perez-Prieto, L. Pastor Perez, M. Gonzalez-Bejar, M. A. Miranda and S. Stribia, *Chem. Comm.*, 2005, 5569-5571.
89. M. X. Wang, H. Yan, X. L. Feng and Y. Chen, *Chin. Chem. Lett.*, 2010, **21**, 1124-1128.
90. J. M. Oton and A. U. Acuna, *Journal of Photochemistry*, 1980, **14**, 341-343.
91. D. Becke, *J Chem. Phys.* 1993, **98**, 5648-5652.
92. C. Lee, W. Yang, and R. G. Parr, *Phys. Rev.*, 1988, **B37**, 785-789.
93. M. J. Frisch, G. W. Trucks, H. B. Schlegel, G. E. Scuseria, M. A. Robb, J. R. Cheeseman, J. A. Montgomery, Jr., T. Vreven, K. N. Kudin, J. C. Burant, J. M. Millam, S. S. Iyengar, J. Tomasi, V. Barone, B. Mennucci, M. Cossi, G. Scalmani, N. Rega, G. A. Petersson, H. Nakatsuji, M. Hada, M. Ehara, K. Toyota, R. Fukuda, J. Hasegawa, M. Ishida, T. Nakajima, Y. Honda, O. Kitao, H. Nakai, M. Klene, X. Li, J. E. Knox, H. P. Hratchian, J. B. Cross, V. Bakken, C. Adamo, J. Jaramillo, R. Gomperts, R. E. Stratmann, O. Yazyev, A. J. Austin, R.

- Cammi, C. Pomelli, J. W. Ochterski, P. Y. Ayala, K. Morokuma, G. A. Voth, P. Salvador, J. J. Dannenberg, V. G. Zakrzewski, S. Dapprich, A. D. Daniels, M. C. Strain, O. Farkas, D. K. Malick, A. D. Rabuck, K. Raghavachari, J. B. Foresman, J. V. Ortiz, Q. Cui, A. G. Baboul, S. Clifford, J. Cioslowski, B. B. Stefanov, G. Liu, A. Liashenko, P. Piskorz, I. Komaromi, R. L. Martin, D. J. Fox, T. Keith, M. A. Al-Laham, C. Y. Peng, A. Nanayakkara, M. Challacombe, P. M. W. Gill, B. Johnson, W. Chen, M. W. Wong, C. Gonzalez, and J. A. Pople, *Gaussian03*, revision Gaussian, Inc.: Pittsburgh, PA, 2003.
94. D. T. Qui, A. Daoud and T. Mhiri, *Acta Crystallagr. Sect. C*, 1989, **45**, 33-35.
95. A. B. P. Lever, E. Mantovani and B. S. Ramaswamy, *Can. J. Chem.*, 1971, **49**, 1957-1964.
96. J. Masternak, B. Barszcz, M. Hodorowicz, O. V. Khavryuchenko and A. Majka, *Spectrochim. Acta A : Mol. Biomol. Spec.*, 2015, **136**, 1998-2007.
97. A. C. Benniston, A. Harriman, D. J. Lawrie, A. Mayeux, K. Rafferty and O. D. Russell, *Dalton Trans.*, 2003, 4762-4769.
98. M. Shiotsuka, Y. Inui, Y. Yamamoto and S. Onaka, *J. Organomet. Chem.*, 2007, **692**, 2441-2447.
99. R. Y. Lai, J. F. Fleming, B. L. Merner, R. J. Vermeij, G. J. Bodwell, and A. J. Bard, *J. Phys. Chem. A*, 2004, **108**, 376-383.
100. R. J. Waltman and J. Bargan, *Can. J. Chem.*, 1986, **64**, 76-95.
101. A. Coleman and M. T. Pryce, *Inorg. Chem.*, 2008, **47**, 10980-10990.
102. E. R. Jamieson and S. J. Lippard, *Chem. Rev.*, 1999, **99**, 2467-2498.
103. S. S. Bhat, A. A. Kumbhar, H. Heptullah, A. A. Khan, V. V. Gobre, S. P. Gejji and V. G. Puranik, *Inorg. Chem.*, 2011, **50**, 545-558.
104. J. B. Lepecq and C. Paoletti, *J. Mol. Biol.*, 1967, **27**, 87-106.

105. A. Goodman, Y. Tseng and W. Denis, *J. Mol. Biol.*, 2002, **323**, 199–215.
106. N. Chowdhury, S. Dutta, S. Dasgupta, N. D. P. Singh, M. Baidyaa and S. K. Ghosh, *Photochem. Photobiol. Sci.*, 2012, **11**, 1239-1250.
107. A. Hussain, S. Gadadhar, T. K. Goswami, A. A. Karande, A. R. Chakravarty, *Eur. J. Med. Chem.*, 2012, **50**, 319–331.
108. S. Dong, H. M. Hwang, C. Harrison, L. Holloway, X. Shi and H. Yu, *Bull. Environ. Contam. Toxicol.*, 2000, **64**, 467-474.
109. E. T. Mack, D. Birzniece, D. R. Veach, W. Coyle and R. M. Wilson, *Bioorg. Med. Chem. Lett.*, 2005, **15**, 2173-2176.
110. S. Li, J. Xiue and D. Shaojun, *J. Photochem. Photobiol. A: Chemistry*, 2006, **18**, 93-97.
111. N. Zhou, Y. Z. Liang and P. Wang, *J. Photochem. Photobiol. A: Chemistry*, 2007, **185**, 271- 276.
112. S. Rajalakshmi, M. S. Kiran, V. G. Vaidyanathan, E. R. A. Singam, V. Subramaniam and B. U. Nair, *Eur. J. Med. Chem.*, 2013, **70**, 280-293.
113. M. Ganeshpandian, R. Loganathan, S. Ramakrishnan, A. Riyasdeen, M. A. Akbarsha and M. Palaniandavar, *Polyhedron*, 2013, **52**, 924-938.
114. A. R. Timerbaev, C.G. Hartinger, S. S. Aleksenko and B.K. Keppler, *Chem. Rev.*, 2006, **106**, 2224-2248.
115. E. Reisner, V. B. Arion, C. G. Hartinger, M. A. Jakupec, A. J. L. Pombeiro and B. K. Keppler in A.M. Trzeciak (Ed.), *Education in Advanced Chemistry*, University of Wroclaw, Wroclaw, 2005, p.215.
116. I. Ascone, L. Messori, A. Casini, C. Gabbiani, A. Balerna, F. Dell'Unto and A. C. Castellano, *Inorg. Chem.*, 2008, **47**, 8629-8634.

117. T. Peters, *Adv. Protein Chem.*, 1985, **37**, 161-245.
118. C. J. Halfman and T. Nishida, *Biochim. Biophys. Acta*, 1971, **243**, 284-293.
119. C. J. Halfman and T. Nishida, *Biochim. Biophys. Acta*, 1971, **243**, 294-303.
120. J. Lakowicz *Principles of Fluorescence spectroscopy*, 1973.